23rd ABCM International Congress of Mechanical Engineering
December 6-11, 2015, Rio de Janeiro, RJ, Brazil

DISSIMILAR RESISTANCE SPOT WELDING OF AISI 1010 CARBON STEEL AND AZ31B MAGNESIUM ALLOY

Frederico Vieira Cintra Karklin Tavares
Guilherme Augusto Ferreira de Macêdo
Paulo Vitor dos Santos Esteves
Soraia Sandra Pires
Thais Roberta Campos
Leonel Dimas de Abreu
Pedro Paiva Brito
Pontifical Catholic University of Minas Gerais, Rua Dom José Gaspar 500, 30535-901 Belo Horizonte (MG)
fredkarklin@hotmail.com, gafmacedo@gmail.com, paulovitor.esteves@hotmail.com, soraiasandrapires@gmail.com, thaisrobertacampos@gmail.com, leonel@pucminas.br, pbrito@pucminas.br

Abstract. *Weight reduction in automotive components can be achieved by the application of light metals, such as magnesium alloys. In turn, the incorporation of such new materials in the existing steel structures demands research and development of joining manufacturing processes. Currently, the most widely used joining process in the automotive industry is resistance spot welding, in which both a limited amount of fusion and plastic deformation take place at the interface to produce a metallurgical bond between the materials. In the present contribution, dissimilar overlap welds of AISI 1010 carbon steel and AZ31B magnesium alloy were produced by resistance spot welding and the resulting joints were analyzed as a function of the welding conditions. Material thickness in both cases was set to 1 mm and the welding experiments were carried out using a conventional spot welder operating with a 8.5 kA welding current. Characterization of the weld microstructure was performed by analyzing the transverse cross section of the joints by conventional optical microscopy and the mechanical properties of the weld nuggets was evaluated by Vickers microhardness. The shear strength of the welded joints was also determined by applying conventional tensile testing. It was possible to observe that, owing to differences in electric and thermal conductivity between both metals, welding with symmetrical (same diameter) electrodes led to excessive melting of steel, overheating of magnesium and puncturing of the AZ31B side of the joint. In order to counter this problem, larger diameter electrodes were employed at the steel side of the joint, reducing current density and improving heat extraction from the weld nugget.*

Keywords: *Resistance Spot Welding (RSW), AISI 1010 carbon steel, AZ31B magnesium alloy, microstructure, mechanical properties.*

1. INTRODUCTION

Increasing energy efficiency of vehicles by reducing weight of structural components is one of the major driving forces for innovative research in the automotive industry today. In this context, it is worth highlighting the incorporation of lightweight materials such as metallic alloys based on aluminum or magnesium in substitution of steel parts. In order to provide an efficient and safe incorporation of light metals in automotive vehicles, it is necessary to adapt or develop joining techniques which allow the union between dissimilar materials without loss of mechanical properties. Resistance Spot Welding (RSW) is the most widely used joining method applied currently in the automotive industry for the production of overlap joints. In this process, a metallurgical bond is formed between the materials by simultaneously applying heat and pressure to the coalescing interface. This is accomplished by the passage of an elevated electric current through the materials, which causes heat dissipation by Joule effect, resulting in a round-shaped weld nugget. The fusion zone is restricted because of the low welding times usually applied (normally fractions of a second). Currently, the RSW process accounts for approximately 90% of joining operations performed on a typical automobile and the total number of spot welds may vary between 7,000 and 12,000 depending on vehicle size and weight (Lang *et al*., 2008). Some of the advantages of the RSW include elevated productivity, good parameter control, and absence of health hazardous fumes or gases, among others.

Magnesium is one of the lightest metals currently employed in structural applications and has drawn attention from researchers in the transport sector. Apart from their low density (1.8 g/cm^3 compared e.g. with 2.7 g/cm^3 for aluminum or 7.87 g/cm^3 for steel), magnesium based alloys can be easily cast for the production of complex parts, have good machinability and strength-to-weight ratio (Froes *et al*., 1997). Liabilities of magnesium alloys, on the other hand, include low room temperature plasticity, elevated chemical reactivity and low high temperature strength (Koike *et al*., 2003). In spite of the potential for weight reduction in structures and the widespread use of the RSW process in the automotive industry, only in the last decade have investigations been performed concerning the dissimilar welding of magnesium and steels (Liu *et al*., 2010; Xu *et al*., 2012; Liu *et al*., 2013; Patel *et al*., 2014).

The dissimilar welding of steel and magnesium alloys using conventional fusion processes constitutes a significant technical challenge because of the large differences in physical properties between the materials, such as electrical and thermal conductivity, coefficient of thermal expansion and melting temperature among others (Liu *et al*., 2010). In this sense, the RSW process presents interesting technical possibilities because of the limited amount of fusion involved, which minimizes residual stresses and the formation of defects such as cracks or pores (Coelho *et al*,. 2012). In the attempt to further advance the knowledge on the microstructure and mechanical properties of dissimilar magnesium-steel joints, in this contribution an investigation of the RSW process applied to joining of AZ31B magnesium alloy and AISI 1010 carbon steel is presented.

2. EXPERIMENTAL PROCEDURE

The materials used in the welding experiments were AZ31B magnesium alloy and AISI 1010 carbon steel sheets with dimensions 1 x 25 x 100. The geometry of the overlap joints is presented in Fig. 1. The welding experiments were performed on a conventional Gregori spot welder with 15kVA power used in previous investigations (Carneiro *et al*., 2005; Brito, 2007). Prior to welding, specimens were ground (400 grit SiC paper) and cleaned in order to remove surface oxides and assist the formation of a metallurgical bond. The effects of contact pressure and current density on the microstructure and mechanical properties of the welded joints were evaluated by applying copper electrodes with varying face diameters. In all cases, the electrodes had a truncated cone geometry, with 45° tip angle.

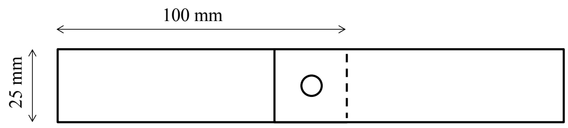

Figure 1. Geometry of the dissimilar overlap joints produced in the present study.

According to previous investigations (Liu *et al*., 2010), dissimilar resistance welding of magnesium to steel using symmetrical (i.e. same geometry) electrodes is inconvenient because of the large discrepancy in physical properties between iron and magnesium, which are presented in Tab. 1.

Table 1. Physical properties of iron and magnesium at 20°C after Liu *et al*. (2010) and Kou (2002)

Element	Melting temperature	Electrical resistivity	Thermal conductivity
Carbon steel	1,538°C	153.0 nΩm	41 $Wm^{-1}K^{-1}$
AZ31B	650°C	44.6 nΩm	96 $Wm^{-1}K^{-1}$

Because of the higher electrical conductivity, higher melting temperature and lower thermal conductivity of steel relative to the magnesium alloy, peak temperatures on the steel side of the joints will be significantly higher than those on the magnesium side which could cause excessive melting of magnesium and the formation of volumetric defects (Liu *et al*., 2010). This was solved by applying larger diameter electrodes on the steel side of the joint in order to reduce current density and increasing cooling rate by heat exchange with the copper electrode (Liu *et al*., 2010). Thus, in the present investigation, electrode face diameter on the steel side was set to 16 mm for all welding conditions whereas the electrode face diameter in contact with the AZ31B alloy was set to 6, 8, 10 and 12 mm.

The welding current, time and voltage drop across the welded interface were, respectively, 8.5 kA, 1 s and 1.5 V. In order to simplify the presentation of results and discussion, samples from the different welding conditions are hereafter referred to as 6-16, 8-16, 10-16 and 12-16 according to the combination of electrode diameters used in each case. It was not possible to obtain mechanically sound welds with the 12-16 condition, since all specimens could be fractured by hand. After welding, adhesion of magnesium to the copper electrodes occurred frequently and these had to be ground and cleaned after each welding operation.

For each viable welding condition, a total of three specimens were selected for tensile testing. Because of the geometry of the overlap joints, the load is not purely tensile, but a bending moment is also present at the interface, thus the tests were not standardized. Metallographic preparation was performed by cutting the materials with an abrasive disc at the center of the weld spot, mounting followed by grinding and polishing. Chemical etching was performed selectively first with 30% diluted solution of acetic acid for 5 min which revealed only the microstructure of the AZ31B material. Examination was performed on the optical microscope and then a 2%Nital solution was applied in order to reveal the steel microstructure. Vickers micro-hardness line profile measurements were performed along the cross section of the welded joints in order to assess hardness variations between Base Material (BM), Heat Affected Zone (HAZ) and Fusion Zone (FZ). The measurements were performed a 0.981 N load and 15 s holding time.

3. RESULTS AND DISCUSSION

3.1 Tensile tests

The results of the tensile tests in terms of load-displacement diagrams for the 6-16, 8-16, 10-16 specimens are presented in Fig. 2(a), (b) and (c), respectively. In the case of the 6-16 sample, only two curves were obtained since one of the specimens fractured during mounting on the tensile testing device (an indication of poor mechanical strength of the welded joint). The data spread is high, denoting difficulties in reproducing welding conditions for each situation.

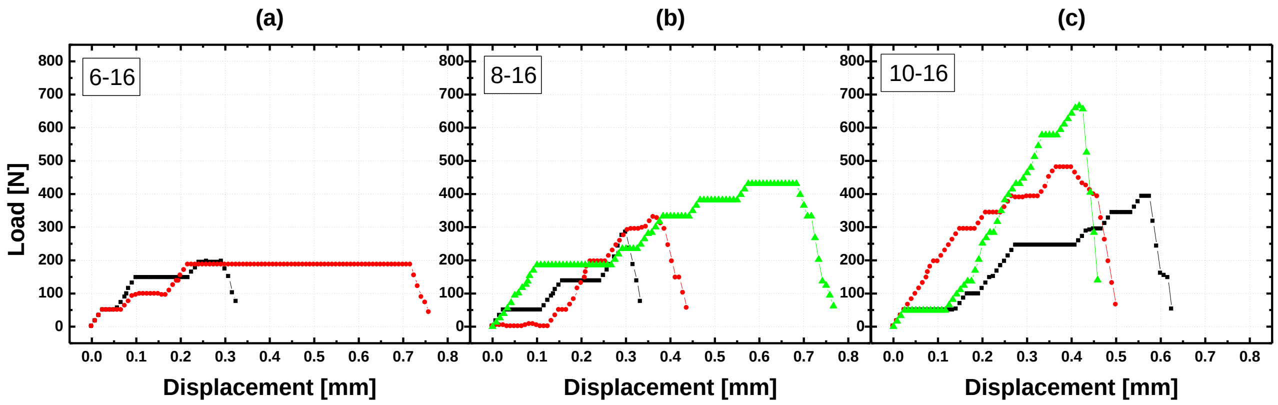

Figure 2. Load-displacement curves from tensile tests performed on the (a) 6-16, (b) 8-16 and (c) 10-16 specimens.

A trend can be noticed showing an increase in mechanical strength (maximum shear load) as a function of electrode diameter on the AZ31B side of the welded joint. This is illustrated in the graphs presented in Fig. 3(a) and (b), which show, respectively, the variation of maximum shear load and toughness (obtained by numerical integration of the load-displacement curves) with respect inverse of the square electrode diameter (D), proportional to welding current density.

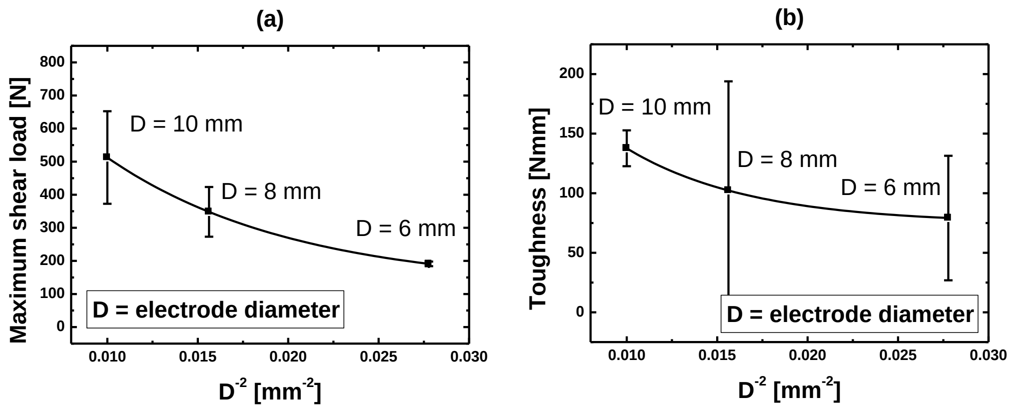

Figure 3. Synthesis of the tensile test results: (a) maximum load and (b) toughness.

The diameter of the weld nuggets from the fractured specimens was determined for the 8-16 and 10-16 samples and the results are presented in Fig. 4. The same results could not be obtained for the 6-16 specimen because of the irregular shape of the nugget, probably caused by overheating and expulsion of magnesium from the welded joint. The results show a positive correlation between tensile strength and toughness and weld nugget diameter, as expected in the RSW process (Chao, 2003). It is important to notice that the failure mechanism that took place during tensile testing of all samples was interfacial fracture instead of pull-out fracture, in which complete withdrawal of the weld nugget is observed. Interfacial fracture is an indication of poor mechanical integrity of the welded joint and is characterized by crack propagation in the weld nugget.

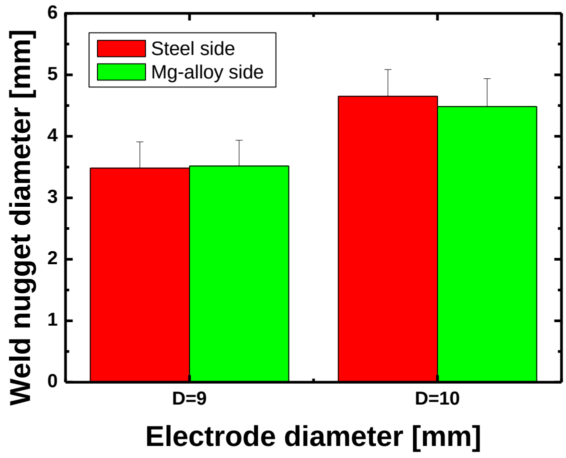

Figure 4. Weld nugget diameter on the steel and Mg-alloy sides of the joints for the 8-16 and 10-16 samples.

3.2 Microhardness profiles

The variation of microhardness along the cross section of the welded joints is presented in Figs. 5 and 6 for the 8-16 and 10-16 samples, respectively. These results were obtained from horizontal profiles on either side of the welds, as indicated. Diagonal microhardness profiles were also obtained for each sample, and these results are presented in Fig. 7.

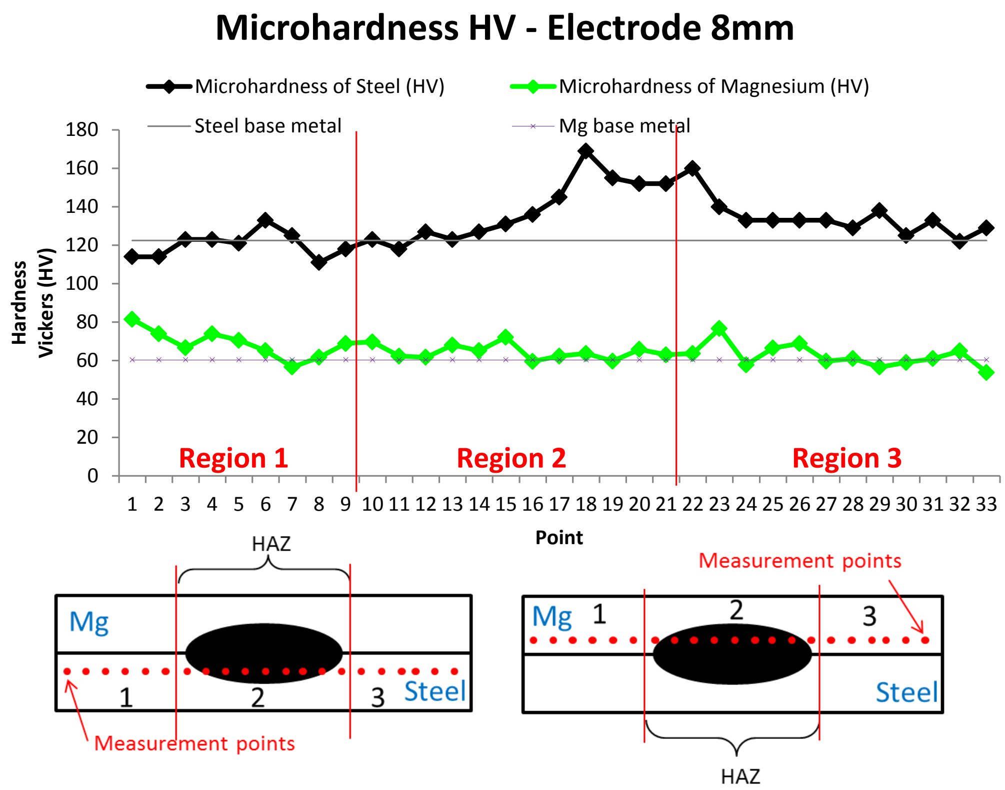

Figure 5. Microhardness profiles determined on the steel and Mg-alloy side of the 8-16 welded joint.

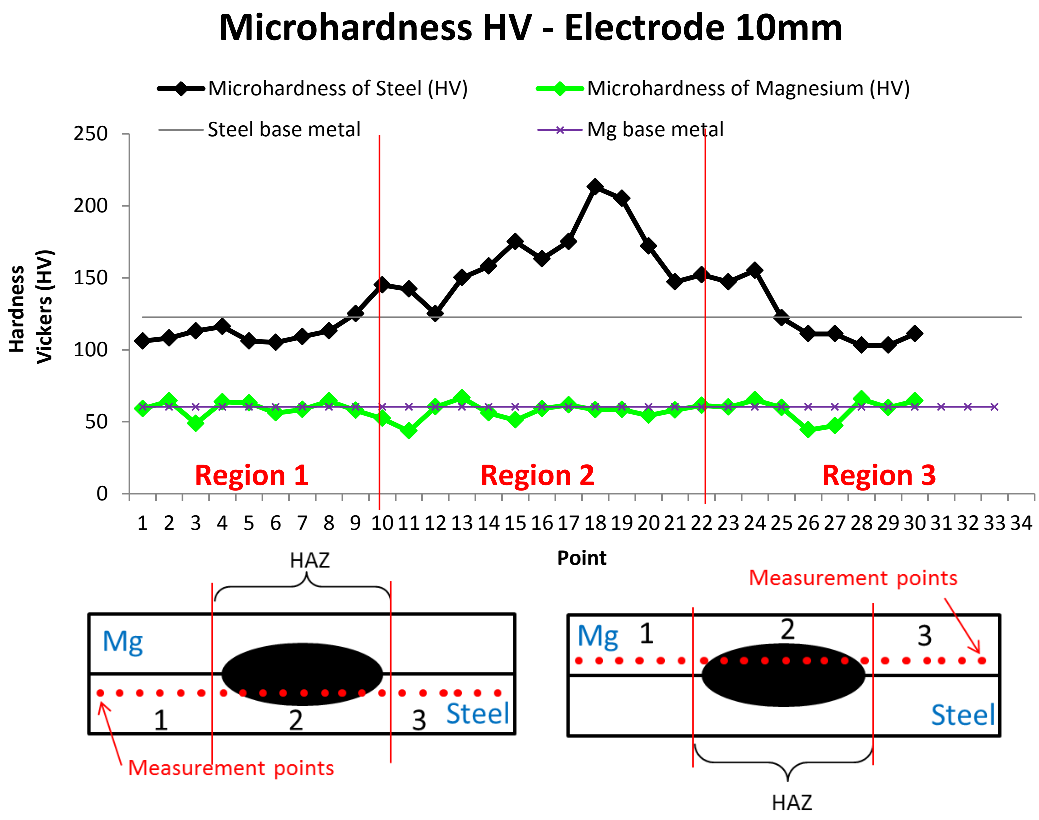

Figure 6. Microhardness profiles determined on the steel and Mg-alloy side of the 10-16 welded joint.

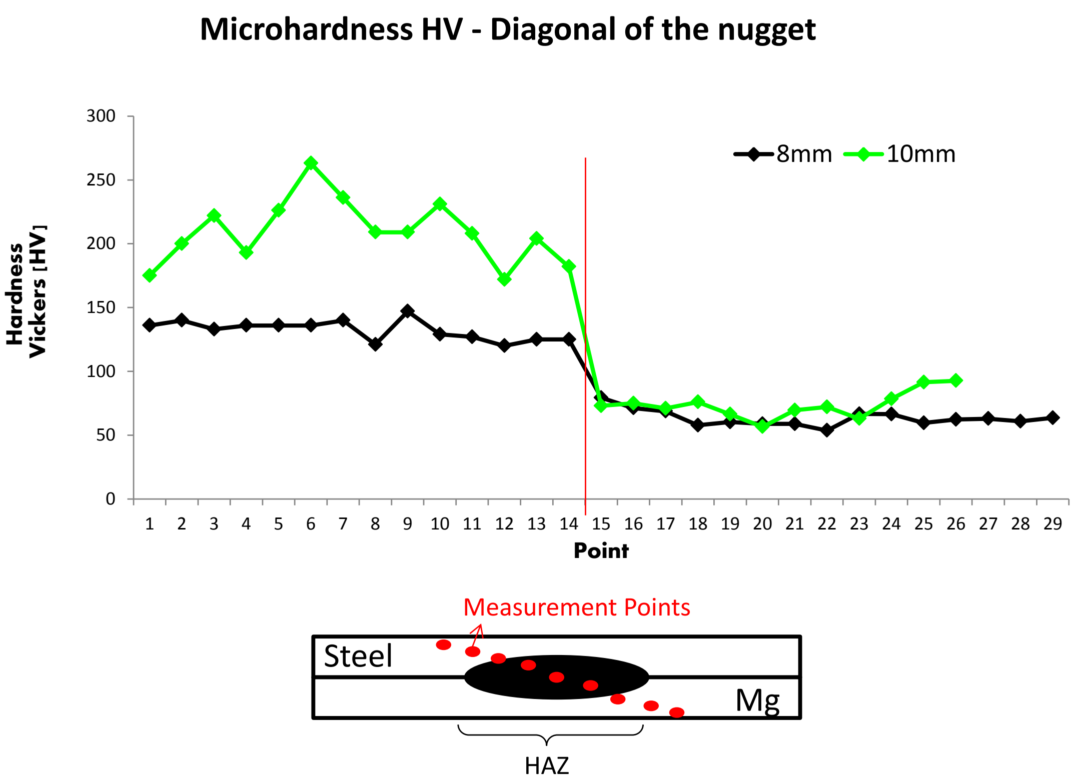

Figure 7. Diagonal microhardness profiles determined across the welded joint cross sections.

The results presented in Figs. 5 and 6 show that for both welding conditions hardness of the AZ31B alloy in the HAZ and FZ does not change relative to values observed in the BM. This is an indication that no significant change in microstructure occurred in the Mg-alloy due to the welding process. The average values obtained were 63.4 and 73.8 HV for the 8-16 and 10-16 samples, while the hardness of the BM prior to welding was 60.3 HV. A different behavior can be observed in the steel side of the welded joints. First, for both the 8-16 and 10-16 samples (Figs. 5 and 6, respectively), an increase in hardness can be noticed in the FZ relative to the values observed in the BM (123 HV). In addition, the maximum hardness values observed in the joints were higher in the 10-16 sample (213 HV) than in 8-16 sample (169 HV). This is probably caused by higher cooling rates due to the larger contact area between metal sheet and copper electrode, leading to the formation of harder constituents in the FZ.

It is important to notice that the microhardness results do not suggest the formation of a diluted zone in the welded joints. This can be seen in the results presented in Fig. 7, which show an abrupt decrease in hardness when the profile transitions from the steel to Mg-alloy side of the joints. Such behavior is consistent with the equilibrium diagram of Fe and Mg, which shows limited room temperature solubility of both elements, as well as an absence of intermetallic compounds (Nayeb-Hasehmi and Clark, 1985).

3.3 Microstructure evaluation

An overview of the welded joint (obtained for the 8-16 sample) is presented in Fig. 8, in which the main regions of the weld can be identified. On both sides of the welded joint, the weld nugget can be visualized by the difference in contrast with the base material. A large number of pits can be seen no the AZ31B side of the joint, which was caused by etching after metallographic preparation.

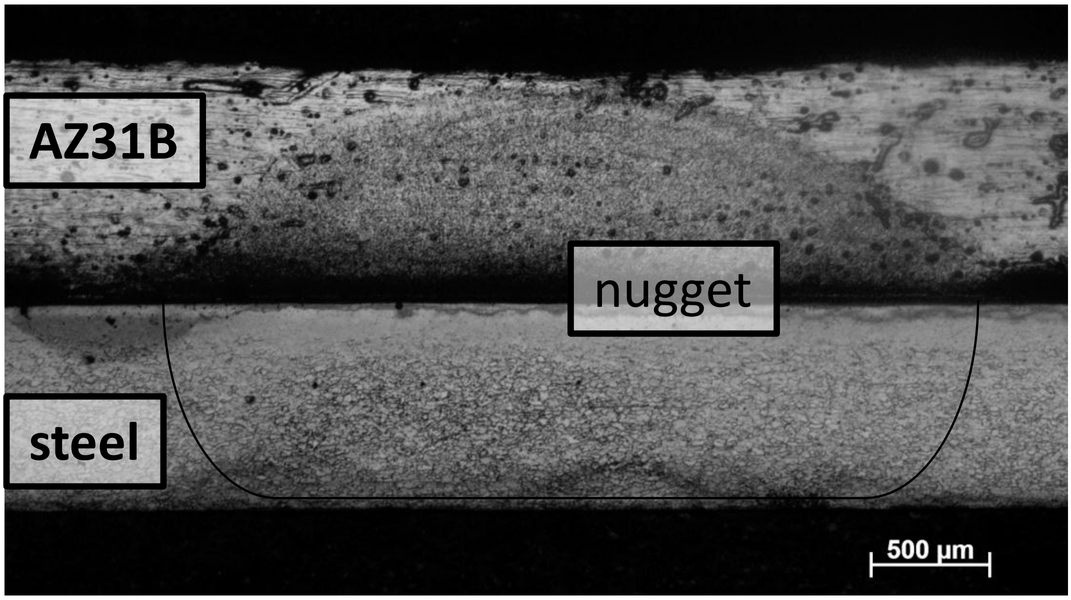

Figure 8. Overview of the weld cross section.

The border of the FZ on the magnesium side of the welded joint is presented in Fig. 9(a) and 8(b) for the 8-16 and 10-16 samples, respectively. Concerning Figure 8(a), the microstructure of the FZ is different from that observed in the HAZ, showing signs of epitaxial growth that stems from the fusion boundary. The most interesting feature of the micrographs presented in Fig. 9 is that there appears to be signs of expulsion of magnesium following the fusion boundary, as indicated by the white arrow in Fig. 9(a). In contrast, the fusion boundary seen in Fig. 9(b) exhibits better cohesion and no signs of volumetric defects. This would lead to loss of mechanical integrity of the weld, in agreement with the mechanical properties results, which showed superior behavior of the welds performed with 10 mm diameter electrodes in contact with the AZ31B side of the welded joint.

The microstructure of the fusion boundary in the steel side of the welded joints is presented in Fig. 10(a) and 10(b) for the 8-16 and 10-16 samples, respectively. The most noticeable difference between the microstructures presented in Fig. 10(a) and (b) is the ferrite and pearlite morphology in the FZ. In the 10-16 sample, Fig. 10(b), the formation of acicular ferrite can be seen whereas in the 8-16 specimen, the grain structure is similar to that observed in the BM and HAZ. The formation of acicular ferrite is associated with higher cooling rates (Kou, 2002), which are expected in the 10-16 specimen because of the larger contact area between workpiece and electrodes. This explains the difference in hardness profiles, presented in Figs. 4-6, and may also be a contribution to the higher mechanical strength observed in the 10-16 samples.

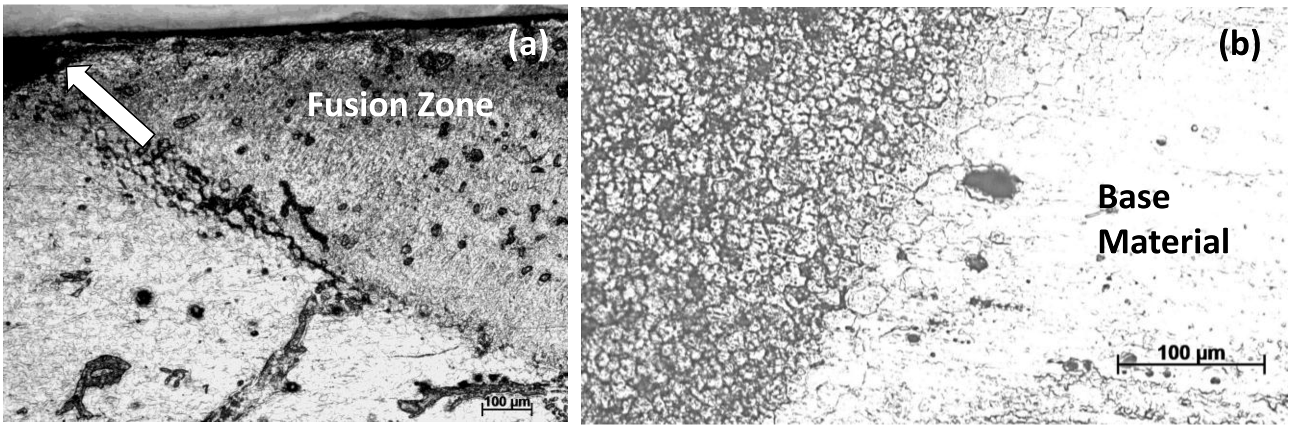

Figure 9. Internal interface between FZ and HAZ on the AZ31B side of the welded joint: (a) 8-16 and (b) 10-16 sample.

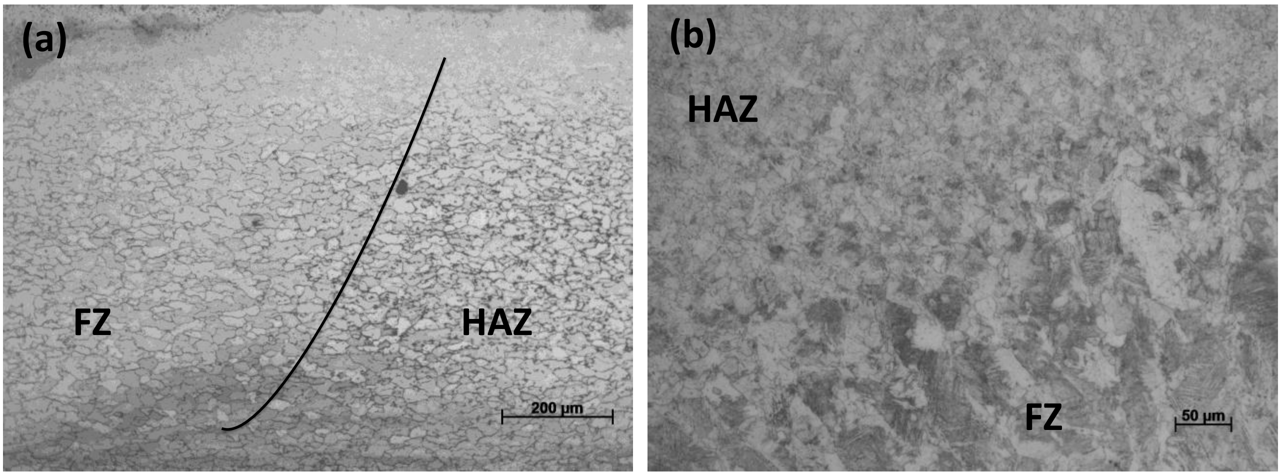

Figure 10. Internal interface between FZ and HAZ on the steel side of the welded joint: (a) 8-16 and (b) 10-16 sample.

4. CONCLUSIONS

In the present contribution, the mechanical properties and microstructure of AISI 1010 low carbon steel and AZ31B magnesium alloy dissimilar joints produced by RSW were investigated. Welding of the two materials with symmetrical (i.e. same diameter) electrodes could not be achieved. Instead, a 16 mm diameter electrode was kept in contact with the steel side of the joint while 6, 8 and 10 mm diameter electrodes applied to the AZ31B alloy side of the joint. The joints produced with the 10 mm electrodes exhibited higher mechanical strength and toughness, which could be associated with two main factors: (i) lower amount of magnesium expulsion and (ii) superior hardness in the steel FZ. In all welding conditions, however, the joints exhibited interfacial failure, an indication of poor mechanical integrity in welds produced by RSW. For this reason, viability of magnesium-to-steel welds must be considered in future studies by variation of other welding parameters such as current, welding time or electrode force.

5. ACKNOWLEDGEMENTS

The authors gratefully acknowledge FAPEMIG (*Fundação de Amparo à Pesquisa de Minas Gerais*) and CNPq (PIBIC) for financial support.

6. REFERENCES

Brito, P.P., 2007. *Influência da força na soldagem por resistência de topo do aço inoxidável AISI 409*. Master thesis, Pontifical Catholic University of Minas Gerais, Belo Horizonte.

Carneiro, J.R.G., Rêgo, A.T., Brito, P. Santana, I.J., 2005. "Automação e monitoração de máquina de solda por pontos para modelagem do perfil de temperatura no aquecimento da soldagem de topo de aço AISI 409". In: *Proceedings of the 3° Congresso de Engenharia de Fabricação*. Joinville, Brazil.

Chao, Y. J., 2003, "Failure mode of spot welds: interfacial versus pullout", *Science and Technology of Welding and Joining*, Vol. 8, p. 133.

Coelho, R.S., Kotska, A., Dos Sanots, J.F., Kaysser-Pyzalla, A., 2012. "Friction-stir dissimilar welding of aluminium to high strength steels: Mechanical properties and their relation to microstructure". *Materials Science and Engineering A*, Vol. 556, p. 175.

Froes, F.H., Eliezer, D. and Aghion, E, 1998. "The Science, Technology and Applications of Magnesium". *Journal of the Minerals, Metals and Materials Society*, Vol. 50, p. 30.

Koike, J., Kobayashi, T., Mukai, T., Watanabe, H., Suzuki, M., Maruyama, K. and Higashi, K, 2003. "The activity of non-basal slip systems and dynamic recovery at room temperature in fine-grained AZ31B magnesium alloys". *Acta Materialia*, Vol. 51, p. 2055.

Kou, S., 2002. *Welding Metallurgy*. John Wiley & Sons, New Jersey; 2nd edition.

Lang, B., Sun, D.Q., Li, G.Z. and QIN, X.F, 2008, "Effects if welding parameters on microstructure and mechanical properties of resistance spot welded magnesium alloy joints". *Science and Technology of Welding and Joining*, Vol. 13, p. 698.

Liu, L., Xiao, L., Feng, J.C., Tian, Y.H., Zhou, S.Q. and Zhou, Y., 2010. "The Mechanisms of Resistance Spot Welding of Magnesium to Steel". *Metallurgical and Materials Transactions A*, Vol. 41, p. 2651.

Liu, L., Xiao, L., Chen, D.L., Feng, J.C., Kim, S. and Zhou, Y., 2013. "Microstructure and fatigue properties of Mg-to-steel dissimilar resistance spot welds". *Materials and Design*, Vol. 45, p. 336.

Nayeb-Hashemi, A.A. and Clark, J.B., 1985. "The Fe-Mg (Iron-Magnesium) System". *Bulletin of Alloy Phase Diagrams*, Vol. 6, p. 235.

Patel, V.K., Bhole, S.D. and Chen, D.L., 2014. "Characterization of ultrasonic spot welded joints of Mg-to-galvanized and ungalvanized steel with tin interlayer". *Journal of Materials Processing Technology*, Vol. 214, p. 811.

Xu, W., Chen, D.L., Liu, L., Mori, H. and Zhou, Y., 2012. "Microstructure and mechanical properties of weld-bonded and resistance spot welded magnesium-to-steel dissimilar joints". *Materials Science and Engineering A*, Vol. 537, p. 11.

7. RESPONSIBILITY NOTICE

The authors are the only responsible for the printed material included in this paper.